NASA TECHNICAL NOTE

NASA TN D-8310 c. 1

COPY: RET
TECHNICAL
KIRTLAND AFB,

TECH LIBRARY KAFB, NM
0134084

NASA TN D-8310

STEADY-STATE HEAT TRANSFER IN TRANSVERSELY HEATED POROUS MEDIA WITH APPLICATION TO FOCUSED SOLAR ENERGY COLLECTORS

Lester D. Nichols

Lewis Research Center
Cleveland, Ohio 44135

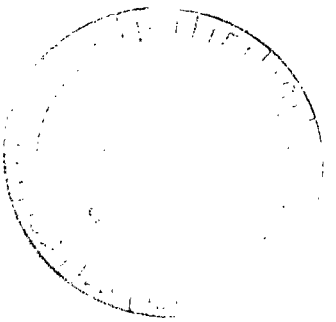

NATIONAL AERONAUTICS AND SPACE ADMINISTRATION • WASHINGTON, D. C. • OCTOBER 1976

TECH LIBRARY KAFB, NM

0134084

1. Report No.	2. Government Accession No.	3. Recipient's Catalog No.
NASA TN D-8310		

4. Title and Subtitle	5. Report Date
STEADY-STATE HEAT TRANSFER IN TRANSVERSELY HEATED POROUS MEDIA WITH APPLICATION TO FOCUSED SOLAR ENERGY COLLECTORS	October 1976
	6. Performing Organization Code

7. Author(s)	8. Performing Organization Report No.
Lester D. Nichols	E-8739
	10. Work Unit No.
	506-24

9. Performing Organization Name and Address	11. Contract or Grant No.
Lewis Research Center National Aeronautics and Space Administration Cleveland, Ohio 44135	
	13. Type of Report and Period Covered
12. Sponsoring Agency Name and Address	Technical Note
National Aeronautics and Space Administration Washington, D.C. 20546	14. Sponsoring Agency Code

15. Supplementary Notes

16. Abstract

A fluid flowing in a porous medium which is being heated transversely to the fluid flow is considered. This configuration is applicable to a focused solar energy collector for use in an electric power generating system. A fluidized bed can be regarded as a porous medium with special properties. The solutions presented are valid for describing the effectiveness of such a fluidized bed for collecting concentrated solar energy to heat the working fluid of a heat engine. Results indicate the advantage of high thermal conductivity in the transverse direction and high operating temperature of the porous medium.

17. Key Words (Suggested by Author(s))	18. Distribution Statement
Heat transfer; Thermal diffusion; Energy absorption; Solar energy conversion; Two-phase flow	Unclassified - unlimited STAR Category 34

19. Security Classif. (of this report)	20. Security Classif. (of this page)	21. No. of Pages	22. Price*
Unclassified	Unclassified	45	$4.00

* For sale by the National Technical Information Service, Springfield, Virginia 22161

STEADY-STATE HEAT TRANSFER IN TRANSVERSELY HEATED POROUS MEDIA WITH APPLICATION TO FOCUSED SOLAR ENERGY COLLECTORS

by Lester D. Nichols

Lewis Research Center

SUMMARY

A fluid flowing in a porous medium which is being heated from a direction that is transverse to the fluid flow is considered. This configuration resembles the design of a focused solar energy collector for use in an electric power generating system. The effect on working fluid outlet temperature of the conductivity of the porous medium, both transverse and parallel to the flow is evaluated, as well as the heat transfer between the fluid and the porous medium.

A fluidized bed can be regarded as a porous medium with special properties. An analysis of a fluidized bed collecting concentrated solar energy to heat the working fluid for a heat engine indicates the advantage of high thermal conductivity in the transverse direction and high melting temperatures of the fluidized material.

The collector will lose heat to the environment from the absorbing surface via both convection and radiation. The radiation loss depends on the emissivity of the surface and can be controlled by use of window materials with appropriate spectral characteristics. The analysis indicates the effect on collector performance of the radiation loss when added to the always present convection loss.

INTRODUCTION

Solar energy can be converted into electrical energy by using it as a heat source for a closed thermodynamic cycle power generating system. The efficiency of such a system improves as the maximum temperature of the working fluid increases. This maximum temperature can be increased by focusing the solar energy but is limited by collector design. Cycles using gas or vapor as a working fluid are the least expensive. However, these working fluids are nearly transparent and cannot absorb the solar energy. In order to use these systems, the collector must be designed to absorb the

solar energy. This is commonly accomplished by an opaque surface. The heat is transferred from the opaque surface to the working fluid by conduction and convection. This step must be carefully considered, because it can introduce large temperature drops between the opaque surface and the working fluid, particularly at high radiant flux levels, and thus decrease system efficiency. Or it can introduce large heat transfer area (and consequently, large equipment size) in order to achieve adequate heat-transfer rates. This will tend to increase capital costs.

A fluidized bed is an excellent candidate for heating a gas working fluid. A fluidized bed is a container of particles through which gas flows from the bottom to the top. The gas velocity is adjusted so the drag force on the particles is equal to the particles' weight, so that the particles levitate. This suspension has many of the properties of a fluid, hence its name. If one of the vertical walls is transparent (fig. 1) then the solar flux can be absorbed by the particles. Fluidized beds have very high effective conductivity (ref. 1), which means large heat-transfer rates from the absorbing surface into the interior where the gas can pick up the energy. Not only that, but the effective conductivity is larger even for materials without large thermal conductivity (e.g., ceramics) which have high melting points. Thus, the use of a fluidized bed to transfer solar energy to a gas may remove the limitations of either low melting temperatures for materials with high conductivity, or low conductivity for materials with high melting points.

A fluidized bed collector can be analyzed as a porous medium with through-flow. In the analysis the temperature of the porous medium and the temperature of the gas are calculated from the energy conservation equations. The three-dimensional, time dependent equations have been derived by Bland (ref. 2). The local velocity must also be specified in these equations. It is specified as proportional to the pressure gradient by using D'Arcy's Law. In heat-transfer cases such as this where the pressure is constant across the flow area, the velocity profile is uniform and the flow is called plug flow.

The coupling between the temperature of the porous medium and the temperature of the flowing gas is dependent on the coefficient of heat transfer. If the coefficient is sufficiently large or particles sufficiently small, then the temperatures will be equal, except in a small region near the gas flow entrance to account for a difference in the boundary condition (ref. 2). Needless to say, this simplifies the analysis considerably by eliminating one of the energy equations.

In this particular application the heat transfer is transverse as well as parallel to the flow direction. This means the analysis must be two dimensional. Not only that, but experiments indicate that the effective conductivity of the fluidized bed is significantly larger in the direction parallel to the flow as compared to the direction transverse to the flow. The analysis must consider a non-isotropic effective thermal

conductivity. But only the steady state is considered. Finally, the boundary conditions on the porous medium for this application specify the heat flux impinging on the surface. They do not specify the temperature of the surface.

Heat transfer between a flowing fluid and a porous medium has been studied intensively. Most of these studies have been one dimensional with the fluid flowing across the surface upon which the heat flux is applied (ref. 3). The application is transpiration cooling. However, there have been some two-dimensional studies. An important application of flow in porous media occurs in geological applications (refs. 4 and 5). The phenomena are complicated and the solutions are numerical. Bland (ref. 2) presented a derivation of the equation for a perfect gas and presented analytical solutions for some special cases, but none for the two-dimensional steady-state case with the heat-flux boundary condition. Siegel and Goldstein (ref. 6) obtained analytical solutions for two-dimensional cases where the fluid is flowing across the surface on which the heat flux is applied with either the heat flux or temperature boundary condition. They treated a variable thickness porous medium and used D'Arcy's law for the velocity of an incompressible gas. But they considered the case where the heat-transfer coefficient between the porous medium and the gas is infinite. Siegel (ref. 7) extended this work to include flow parallel to the heat flux surface (i.e., a coolant passage). However, he obtained solutions for only the case of a specified surface temperature and not the specified heat flux. Koh and Colony (ref. 8) considered the two-dimensional problem with the heat flux specified for plug flow in a channel of constant cross sectional area without assuming the heat-transfer coefficient between the gas and the porous media to be infinite. However, they did not consider nonisotropic conductivity and obtained only numerical solutions.

In this report the steady-state solution to the two-dimensional problem with heat flux boundary conditions and a finite heat-transfer coefficient is obtained. Plug flow in a constant area flow passage and constant specific heat and thermal conductivity is assumed. The thermal conductivity can, however, be nonisotropic. Solutions are also obtained for limiting values of the parameters. An appropriate limiting solution is then used to evaluate the absorber as the heat source for a Carnot thermodynamic cycle. Calculations illustrate the advantage of the trade-off between absorber high melting point and high thermal conductivity and the effect of collector losses to the environment.

ANALYSIS

Governing Equations

Consider a porous medium contained in a transparent walled container as shown in figure 1. This container is the radiation absorber. A flux Φ impinges on the trans-

parent wall, passes through the wall, and is absorbed by the solid material. The absorbed energy is conducted away from the transparent wall in the porous media, and transferred to the gas flowing in the pores by convection. Some is lost from the porous medium to the environment. The heat conduction parallel to the flow is assumed to be different from the heat conduction perpendicular to the flow. The steady-state energy balance equation for the gas in plug flow is (ref. 9, p. 530, eq. 42-1)

$$(\rho u)_o c_p \frac{\partial t}{\partial z} = k_{sx} \frac{\partial^2 t_s}{\partial x^2} + k_{sz} \frac{\partial^2 t_s}{\partial z^2} \tag{1}$$

(The symbols are defined in appendix A.)

This equation is valid when the chosen coordinates coincide with the axes of principle thermal conductivity (ref. 10, p. 14). Such will be the case for a fluidized bed oriented with the z axis parallel to the body force. The conductivity of the medium in both directions is an effective conductivity. It depends not only on the type of medium but also the type of gas (ref. 11). Heat conduction by the gas is neglected since the effective conductivity in the medium is typically 10 times that of the gas (ref. 11). There is no net motion of the solids. The steady-state energy balance for the medium is (ref. 9, p. 530, eq. 42-2)

$$k_{sx} \frac{\partial^2 t_s}{\partial x^2} + k_{sz} \frac{\partial^2 t_s}{\partial z^2} = \frac{Sh_s}{V} (t_s - t) \tag{2}$$

Boundary Conditions

The gas temperature at the entrance (z = 0) will be given as t_o. The boundary conditions specified on the porous medium is the heat flux. At the entrance (z = 0) and the exit (z = L), the heat is transferred from the porous medium to the gas by convection. The boundary condition should be (ref. 12):

$$k_{sz} \left.\frac{\partial t_s}{\partial z}\right|_{z=0} = h_o(t_s - t_o) \qquad k_{sz} \left.\frac{\partial t_s}{\partial z}\right|_{z=L} = h_{ex}(t_{ex} - t_s)$$

Integrating equation (1) and applying these boundary conditions indicates that if

$$\frac{(\rho u)_o c_p}{h_o} >> \frac{t_s}{t_o} - 1 \qquad \text{at } z = 0$$

and

$$\frac{(\rho u)_o c_p}{h_{ex}} >> 1 - \frac{t_e}{t_{ex}} \qquad \text{at } z = L$$

then the energy lost by the porous medium end surfaces to the gas is negligible compared with the energy picked up by the gas from the porous media volume. These inequalities apply for all cases considered herein so that only a small error is introduced when boundary conditions are

$$\left.\frac{\partial t_s}{\partial z}\right|_{z=0} = 0 \quad \text{and} \quad \left.\frac{\partial t_s}{\partial z}\right|_{z=L} = 0$$

We will consider only this boundary condition in the z direction. In the x direction no heat will be lost from the porous medium along the insulating plane (x = 0). However, at the absorbing surface, (x = B) the absorbed energy will be either conducted inward or lost to the environment:

$$k_{sx} \left.\frac{\partial t_s}{\partial x}\right|_{x=B} + h_w(t_s - t_{env}) = \Phi \tag{3}$$

Nondimensional Variables and Parameters

Introduce the following variables:

$$\xi \equiv \frac{x}{B} \qquad \zeta \equiv \frac{z}{L} \tag{4}$$

$$\varphi(\xi, \zeta) \equiv \frac{h_w\left[t(x, z) - t_{env}\right] - \Phi}{h_w(t_o - t_{env}) - \Phi}$$

$$\psi(\xi,\zeta) \equiv \frac{h_w\left[t_s(x,z) - t_{env}\right] - \Phi}{h_w(t_o - t_{env}) - \Phi}$$

and parameters

$$\beta \equiv \frac{SB}{V}\frac{h_s}{h_w} \qquad \omega \equiv \frac{(\rho u)_o c_p B}{L h_w} \qquad \nu \equiv \frac{k_{sx}}{B h_w} \qquad \mu \equiv \frac{k_{sz}}{L h_w}\left(\frac{B}{L}\right) \tag{5}$$

into equations (1) and (2). The equations and boundary conditions become

$$\omega\varphi_\zeta = \nu\psi_{\xi\xi} + \mu\psi_{\zeta\zeta} = \beta(\psi - \varphi) \tag{6}$$

$$\varphi(\xi, 0) = 1 \tag{7}$$

$$\psi_\xi(0, \zeta) = 0 \tag{8}$$

$$\nu\psi_\xi(1, \zeta) + \psi(1, \zeta) = 0 \tag{9}$$

$$\psi_\zeta(\xi, 0) = \psi_\zeta(\xi, 1) = 0 \tag{10}$$

General Solution

The separation of variables technique will be used to get the solutions.[1] Assume solutions of the form

$$\varphi = \sum_{n=0}^{\infty} a_n(\zeta)\cos\,\alpha_n\xi \tag{11}$$

$$\psi = \sum_{n=0}^{\infty} b_n(\zeta)\cos\,\alpha_n\xi \tag{12}$$

Equations (8) and (9) are satisfied if

[1]This technique was used by Bland (ref. 2) to solve a time dependent problem with one space coordinate. His solutions are the same as herein if $k_{sx} = k_{sz}$ and $x = u_o\tau$ where τ is time. However, he considers different boundary conditions.

$$\nu\alpha_n \sin \alpha_n = \cos \alpha_n \qquad n = 0, 1, 2, \ldots \tag{13}$$

Substitute φ and ψ from equations (11) and (12) into equation (6):

$$\sum_{n=0}^{\infty} (\omega a_n' - \beta b_n + \beta a_n)\cos \alpha_n \xi = 0 \tag{14}$$

$$\sum_{n=0}^{\infty} (\omega a_n' - \mu b_n'' + \nu \alpha_n^2 b_n)\cos \alpha_n \xi = 0 \tag{15}$$

These equations must be valid for all ξ; hence,

$$\omega a_n' - \beta b_n + \beta a_n = 0 \tag{16}$$

$$\omega a_n' + \nu \alpha_n^2 b_n - \mu b_n'' = 0 \tag{17}$$

This set of equations possesses solutions of the form

$$a_n = A_n e^{\gamma_n \zeta} \quad \text{and} \quad b_n = B_n e^{\gamma_n \zeta} \tag{18}$$

where

$$\frac{A_n}{B_n} = \frac{\beta}{\beta + \omega\gamma_n} \tag{19}$$

and

$$\omega\beta\gamma_n = (\beta + \omega\gamma_n)(\mu\gamma_n^2 - \nu\alpha_n^2) \tag{20}$$

Equation (20) is a cubic equation in γ_n and is the same as equation (71) in Bland (ref. 2). There are three roots. Let $\gamma_n^{(i)}$ denote the i^{th} root. Then equations (11) and (12) can be written as

$$\varphi = \sum_{n=0}^{\infty} \sum_{i=1}^{3} A_n^{(i)} e^{\gamma_n^{(i)} \zeta} \cos \alpha_n \xi \tag{21}$$

and

$$\psi = \sum_{n=0}^{\infty} \sum_{i=1}^{3} A_n^{(i)} \frac{\beta + \omega \gamma_n^{(i)}}{\beta} e^{\gamma_n^{(i)} \zeta} \cos \alpha_n \xi \tag{22}$$

There are three boundary conditions that still must be satisfied: The two in equation (10) require

$$\sum_{i=1}^{3} \left[\beta + \omega \gamma_n^{(i)}\right] \gamma_n^{(i)} A_n^{(i)} = 0 \tag{23}$$

$$\sum_{i=1}^{3} \left[\beta + \omega \gamma_n^{(i)}\right] \gamma_n^{(i)} e^{\gamma_n^{(i)}} A_n^{(i)} = 0 \tag{24}$$

and equation (7) requires

$$\sum_{n=0}^{\infty} \sum_{i=1}^{3} A_n^{(i)} \cos \alpha_n \xi = 1 \tag{25}$$

But, since the eigenfunctions are orthogonal on the interval 0 to 1, equation (25) can be put into the form of equations (23) and (24) by multiplying by $\cos \alpha_m \xi$ and integrating over the interval 0 to 1 and only terms $m = n$ remain:

$$\sum_{i=1}^{3} A_n^{(i)} = \frac{2 \sin \alpha_n}{\alpha_n + \sin \alpha_n \cos \alpha_n} \equiv M_n \tag{26}$$

Equations (23), (24), and (26) represent three equations for the three unknowns $A_n^{(1)}$, $A_n^{(2)}$, and $A_n^{(3)}$. The solutions are

$$D_n A_n^{(1)} = M_n \gamma_n^{(2)} \left[\beta + \omega \gamma_n^{(2)}\right] \gamma_n^{(3)} \left[\beta + \omega \gamma_n^{(3)}\right] \left[e^{\gamma_n^{(3)}} - e^{\gamma_n^{(2)}}\right] \tag{27}$$

$$D_n A_n^{(2)} = M_n \gamma_n^{(1)} \left[\beta + \omega \gamma_n^{(1)}\right] \gamma_n^{(3)} \left[\beta + \omega \gamma_n^{(3)}\right] \left[e^{\gamma_n^{(1)}} - e^{\gamma_n^{(3)}}\right]$$

and

$$D_n A_n^{(3)} = M_n \gamma_n^{(1)} \left[\beta + \omega \gamma_n^{(1)}\right] \gamma_n^{(2)} \left[\beta + \omega \gamma_n^{(2)}\right] \left[e^{\gamma_n^{(2)}} - e^{\gamma_n^{(1)}}\right]$$

where

$$D_n \equiv e^{\gamma_n^{(1)}} \gamma_n^{(1)} \left[\beta + \omega \gamma_n^{(1)}\right] \left[\gamma_n^{(3)} - \gamma_n^{(2)}\right] \left[\gamma_n^{(3)} \omega + \gamma_n^{(2)} \omega + \beta\right] + e^{\gamma_n^{(2)}} \gamma_n^{(2)} \left[\beta + \omega \gamma_n^{(2)}\right] \left[\gamma_n^{(1)}\right.$$

$$\left. - \gamma_n^{(3)}\right] \left[\gamma_n^{(1)} \omega + \gamma_n^{(3)} \omega + \beta\right] + e^{\gamma_n^{(3)}} \gamma_n^{(3)} \left[\beta + \omega \gamma_n^{(3)}\right] \left[\gamma_n^{(2)} - \gamma_n^{(1)}\right] \left[\gamma_n^{(2)} \omega + \gamma_n^{(1)} \omega + \beta\right] \tag{28}$$

In this way the solutions for φ and ψ are given by equations (21) and (22) with the α_n's given in equation (13), the $\gamma_n^{(i)}$'s given by equation (20), and the $A_n^{(i)}$'s given in equations (27) and (28). Solutions are presented in appendix D for limiting values of some of the parameters.

There are two numbers which are important in the application of porous medium collectors: the amount of heat picked up by the gas and the maximum temperature of the porous medium. The heat transferred to the gas increases the average temperature of the gas, which is defined as

$$\langle t \rangle \equiv \frac{1}{B} \int_0^B t(x, z)\, dx \tag{29}$$

Then the average temperature from equation (11) is

$$\frac{\langle t\rangle - t_o}{\Phi/h_w + t_{env} - t_o} = 1 - \sum_{n=0}^{\infty} a_n(\xi)\frac{\sin \alpha_n}{\alpha_n} \tag{30}$$

The maximum temperature of the porous media, $t_{max} = t\ (x = B,\ z = L)$ can be written from equation (12) as

$$\frac{t_{max} - t_o}{\Phi/h_w + t_{env} - t_o} = 1 - \sum_{n=0}^{\infty} b_n(1)\cos \alpha_n \tag{31}$$

COLLECTOR PERFORMANCE AS THE HEAT SOURCE FOR A CARNOT CYCLE

The collector analyzed herein can be considered as the heat source for any closed thermodynamic cycle. The various collector parameters and their effects on the efficiency of such a system when the closed thermodynamic cycle is a Carnot cycle (or has an efficiency that is a fixed fraction of a Carnot cycle) are studied. The efficiency of a Carnot cycle operating between the average temperature of the gas at the outlet of the collector and the temperature of the environment is calculated.

The fraction of the power impinging on the collector that is collected by the gas is

$$\eta_{coll} = \frac{(\rho u)_o c_p B(\langle t\rangle - t_{env})}{\Phi L} \tag{32}$$

and the efficiency of a system with Carnot efficiency is

$$\eta = \eta_{coll}\frac{\langle t\rangle - t_{env}}{\langle t\rangle} \tag{33}$$

This can be written in terms of ω (eq. (5)) and Θ where

$$\Theta \equiv \frac{\Phi}{h_w t_{env}} \tag{34}$$

as

$$\eta = \frac{\omega}{\Theta} \frac{(\langle t \rangle - t_{env})^2}{t_{env}\langle t \rangle} \tag{35}$$

It is the intention here to determine the maximum efficiency possible for a collector of given size and of a given porous medium. Intuitively one expects this to occur at the maximum amount of heat that the gas can absorb. Therefore, the temperature of the gas and the porous medium are assumed to be the same at the exit of the collector. This can be achieved if L is large. Just how large will be shown later. The conductivity of the porous medium in the direction parallel to the gas flow is assumed to be infinite. This restriction will tend to lower the exit gas temperature (since the porous medium will be at a constant temperature in the parallel direction) but is consistent with the properties of a fluidized bed.

Under these two conditions the limiting solutions are obtained in appendix D as

$$t = t_s + (t_s - t_{env})e^{-\beta\zeta/\omega} \tag{36}$$

and

$$t_s = t_{env} \{1 + C \cosh \chi\xi\} \tag{37}$$

where χ is defined in equation (D9) and all boundary conditions except equation (3) are satisfied. This boundary condition relates the heat flux to the collector characteristics. In appendix D, C is evaluated using equation (3) when the heat loss from the collector to the environment is by convection only. However, at high collector temperature, heat loss to the environment may be dominated by radiation. In this case the boundary conditions should be

$$k_{sx} \frac{dt_s}{dx} + \epsilon\sigma\left(t_s^4 - t_{env}^4\right) = \Phi \tag{38}$$

If

$$h_w = 4\epsilon\sigma t_{env}^4 \tag{39}$$

the equation to determine C becomes

$$C\nu\chi \sinh \chi + \frac{1}{4}\left\{(1 + C \cosh \chi)^4 - 1\right\} = \Theta \tag{40}$$

This definition of h_w is chosen so that, when t_s is only slightly different from t_{env}, equation (38) will reduce to equation (3). Equation (40) defines C which in turn defines t_s. The average temperature of the gas leaving the collector is

$$\langle t \rangle = t_{env} \left\{ 1 + \frac{C \sinh \chi}{\chi} \right\} \tag{41}$$

If all the parameters are fixed except the mass flow parameter, there is an optimum value of the mass flow parameter that maximizes the efficiency. This optimum occurs because, when the mass flow is too low, the collector transfers a very small amount of heat to the gas and the collector losses are a large fraction of the impinging flux. On the other hand, at large values of the mass flow parameter, the exit temperature of the gas is low and the efficiency of the Carnot cycle is very low. The calculations for the performance of the collector as a heat source for a thermodynamic cycle will be made at this optimum value of the mass flow parameter.

CALCULATION PROCEDURE

It is necessary to evaluate the eigenvalues from equation (13) in order to obtain numerical answers from the solutions given in equations (21) and (22). These eigenvalues were obtained using the numerical technique described in appendix B. After calculating each eigenvalue, it is necessary to obtain all three roots of the cubic equation (20). The procedure used in the calculation, along with some limiting values, is shown in appendix C. The calculations were made on a desk calculator, which had been equipped with additional memory.

RESULTS AND DISCUSSION

To discuss the effect of some parameters on the average outlet gas temperature and the maximum porous medium temperature, let us consider certain of the parameters as fixed. Consider a given radiative absorber size (fixed L and B) with a specified heat-transfer parameter to the environment h_w. We will then look at the effects of fluid-particle heat transfer, parallel and transverse porous medium conductivity, and the mass flow of gas passing through the absorber. Many studies of flow in porous media have assumed that the heat-transfer coefficient between the gas and the medium is infinite. This means that the gas and medium temperatures are equal (except in a small entrance region). First the condition under which this assumption is valid in so far as

its effect on the average gas temperature at the absorber exit is concerned is examined.

Mass Flow Parameter Chosen Independently

Effects of heat-transfer coefficient. - In figure 2 the average exit gas temperature and maximum temperature of the porous medium are examined for three different values of the mass flow parameter. The transverse and parallel conductivity parameters are set equal. Consider first figure 2(a) where the conductivity parameters are 0.01. There is a value of β (depending upon ω) beyond which further increases have negligible effect on either the maximum temperature of the porous medium or the average gas temperature. This value is about 8ω. Examination of figure 2(b) for conductivity parameters of 1.0 reveals the same conclusion. As a matter of fact, equations (D3) and (D4) show the same results when μ and ν become infinite. And equations (D11) and (D12) show the same thing when only μ is infinite. This condition can be related to a minimum desirable length of the absorber. The condition $\beta > 8\omega$ can be written as $L > 8(\rho u)_o c_p V/Sh_s$ for a fluidized bed of spheres, where the void fraction is taken to be 0.4. A good approximation for the gas-to-particle heat-transfer coefficient for gases with Prandtl number of 1, and particle Reynolds numbers greater than 1 is (ref. 13, p. 215)

$$h_s = \frac{1}{20}(\rho u)_o c_p$$

Substituting the surface to volume ratio and heat-transfer coefficient into the minimum length requirement yields the following relation:

$$L > 45\, d_s$$

Effect of parallel conductivity of porous medium. - To examine the effects of the parallel conductivity parameter, take, for example, the case of reasonably thick collectors in the atmosphere where $\beta = 100$ might be typical. A reasonably high conductivity in the transverse direction (say copper) would yield $\nu = 100$. For these parameters the effect of mass flow on both the average gas temperature and the maximum solid medium temperature is shown in figure 3(a) for three values of the ratio of parallel conductivity to wall heat loss. Notice that high average temperature requires low mass flow rates. Also, note that, as the ratio of parallel to transverse conductivity increases, the average temperature decreases (except at the extreme limits of no temperature increases or no gas flow into the absorber). Note finally that there can be a difference in

temperature between the maximum porous medium temperature and the average gas temperature (except in the limit of no mass flow into the absorber).

Now consider an abosrber with a transverse conductivity which is much smaller than the previous absorber, say porous alumina. A typical value here might be $\nu = 1$. The same parameters are shown for this absorber in figure 3(b). For this case the temperature difference between the average gas temperature and the maximum porous medium temperature is negligible. A comparison of figures 3(a) and (b) reveals that the effect of the poorer solid conductivity can be compensated for by reducing the mass flow so that the same fluid average temperature can be maintained. The curves in figure 3 were calculated using the general solution. However, as the parallel conductivity parameter μ becomes larger, the limiting form of the solution obtained in appendix D can be used. At $\mu = 100$ the two solutions are indistinguishable (fig. 3).

Effect of transverse porous medium conductivity. - In figure 4 the dimensionless values of the average exit gas temperature and maximum porous medium temperature are shown for three different values of the mass flow parameter. The heat-transfer parameter β is 100 and the transverse and parallel thermal conductivity parameters are equal. At low values of the transverse conductivity, a significant difference between the maximum and average temperature exists. However, the difference become less than a few percent for values of the transverse conductivity parameter greater than $\sqrt{10\omega}$. As a matter of fact, when this condition is met, the limiting solution given in appendix D (eqs. (D3) and (D4)) is correct. Thus, for equal transverse and parallel conductivity parameters, the condition specifies a minimum value of the conductivity parameter for which the transverse temperature gradients can be neglected. Larger values are unnecessary. This implies that for a given porous material the thickness B need be no smaller than some minimum value (see eq. (5)).

Effect of mass flow. - In figure 5 the dimensionless values of the average exit gas temperature and the maximum porous medium temperature are shown as a function of mass flow parameter for several values of the transverse conductivity parameter. Again, the heat-transfer parameter β is 100. However, the parallel porous medium conductivity parameter μ is taken as infinite. This is a reasonable approximation for a fluidized bed with L/B less than 10. In this case, the limiting form of the solution as given in appendix D (eqs. (D11) and (D12)) is valid and is used in making the calculation. Once again, a minimum value of the transverse conductivity parameter for which the transverse temperature gradients can be neglected is found. The value is 10 and, in turn, specifies a minimum thickness for the porous medium when a material is selected.

Up to now the mass flow parameter has been assumed to be independent. We have found that the average temperature of the gas leaving the absorber does not change when the collector length exceeds a certain value, when the collector width becomes smaller

than a certain value, or when the ratio of parallel to transverse conductivity exceeds a certain value. Some of these limiting values depend on the mass flow parameter value. For certain applications there may be other considerations which are important and they dictate that a certain mass flow parameter be used. In this case the mass flow parameter will no longer be independent. One such application is using the collector to heat the working fluid for a closed thermodynamic cycle.

Mass Flow Parameter Dependent On Heat Flux and Transverse Conductivity Parameters

Consider the collector as the working fluid heater for a closed thermodynamic cycle with Carnot efficiency or a fixed fraction of Carnot efficiency. Intuitively, one feels that this heater should be designed to have a minimum temperature difference between the porous medium and the average temperature of the gas leaving the heater. This implies a collector length greater than some minimum (in the case of spherical particles it is 45 d_s). If it is assumed that that condition is satisfied, an infinite heat-transfer parameter can be used to make calculations.

The large effective conductivity of a fluidized bed makes it attractive for this application. The parallel conductivity in a fluidized bed is much larger than the transverse. For beds with length to width ratios no greater than 10, the transverse conductivity parameter μ will be large. As long as it is larger than 10, the calculations can be made assuming the parameter is infinite. Thus, all calculations will be made using this limiting solution.

The effect of the two remaining parameters, the transverse conductivity parameter ν and the heat flux parameter Θ, is now considered. The mass flow parameter will be expressed in terms of these two remaining parameters. It will be determined as being the value that maximizes the cycle efficiency.

The efficiency of the cycle also depends on the type of loss from the collector to the environment. All collectors will have a convection loss which depends on their surface temperatures and the conditions of the environment. In addition, there may be radiation losses to the environment. These losses can become large as the surface temperature increases, but they can be counterracted by using a low emissivity surface. This can be accomplished to some degree by using a window that transmits the short wave length incoming flux and reflects the longer wave length outgoing flux. In this way, even though the collector has a high absorptivity, its emissivity may be small, and the window may reflect the absorber's emitted energy back. The window losses to the environment would then be governed by convection, even at high temperatures. In order to consider the effect of this option, two cases are presented. The first is a case with convection only, regardless of collector temperature. The second is a case with radiation only,

regardless of collector temperature. However, in the second case, the emissivity of the radiating surface is assumed to be adjusted so that at low surface temperatures, the radiant heat loss is numerically equal to the convective heat loss. The radiating surface is assumed to be at the same temperature as the collector surface.

The efficiency is calculated for a Carnot cycle, with losses to the environment by convection only, as a function of mass flow parameter (fig. 6). There are two different values of transverse conductivity parameter and three different values of the heat flux parameter. Note that there is a value of mass flow parameter that maximizes the cycle efficiency and that its value depends on the remaining two parameters. All subsequent calculations of collector performance assume that the mass flow parameter is optimum. The effects of varying the two independent parameters on the cycle efficiency and the optimum mass-flow-rate parameter are investigated. And these quantities are plotted as functions of the ratio of the maximum temperature of the porous medium to the environment temperature. This method of presentation is then useful when comparing the two different types of collector losses for the same porous medium.

The calculations for the efficiency are shown in figure 7 for the two heat loss conditions and illustrate the expected results that as the ratio of medium to environment temperature increases and the conduction parameter increases the efficiency increases. The efficiency approaches a maximum value monotonically for the convection condition as the flux parameter increases for a fixed value of the conductivity parameter. However, for the radiation-loss case (fig. 7(b)), there is a maximum efficiency as the flux parameters increase for fixed values of the conductivity parameter.

As one expects intuitively, at a given value of the heat flux parameter, the efficiency for the convection boundary condition is better than for the radiation condition - regardless of the value of the conductivity parameter. However, for a given ratio of medium to environment temperature, the efficiency with the radiation-loss condition is higher than with the convection-loss condition, if the conduction parameter is large enough. These higher efficiencies, however, require much larger heat flux parameters. Comparing figures 8(a) and (b) shows that much larger mass flow parameters are also required for the radiation loss. Thus, even though the heat losses per unit receiver area are larger (at a fixed porous medium temperature) with the radiation-loss condition, the total area required is smaller. This is true because of the higher mass flow rates required at the high heat flux values. The result is that a larger fraction of the incoming flux is transferred to the gas.

To achieve these high efficiencies, a very large value of the heat conduction parameter is also required. Because of its high effective conductivity, a fluidized bed of particles can attain the needed value in a bed which is much thicker than a packed bed using copper. Also, if the particles are made of a material with high melting temperature, the efficiency of the system can also be improved by operating at a higher temperature.

PERFORMANCE OF A SOLAR COLLECTOR

The performance characteristics of solar collectors using porous copper and fluidized alumina are compared in figure 9. The length L to thickness ratio B for all collectors is 10. The two heat-loss boundary conditions are shown for one temperature ratio (3) for copper and the radiation-loss condition for three temperature ratios (3, 4, 5) for the fluidized alumina. Results are shown for three thicknesses: 0.1, 1, and 10 meters. The conductivity is 70 watts per meter per kelvin for sintered porous copper (ref. 14) and 800 watts per meter per kelvin for the fluidized alumina (ref. 1). The heat-transfer coefficient is 9.3 watts per square meter per kelvin for convection (ref. 15, p. 529), and 8.1 watts per square meter per kelvin for radiation with an environment temperature of 330 K. The first is the natural convection coefficient for a long vertical flat plate in air, and the second is for a black absorber at the environment temperature.

Some trends and conclusions from these comparisons are as follows. Figure 9(a) shows that absorber thicknesses on the order of a meter for the fluidized alumina provides the same efficiency as copper with thicknesses on the order of 0.1 meter. This implies larger mass flow and lower capital cost. At a temperature ratio of 3 and a thickness of 0.1 meter for copper, the efficiency for both the convection and radiation loss cases are about the same; however, at larger thickness the efficiency of the system with the radiation boundary condition drops off rapidly. Generally, a system has higher efficiency if the temperature ratio is high and the thickness small.

The heat flux which must be applied to achieve the efficiencies is shown in figure 9(b). For a radiant flux of 640 kilowatts per square meter (used for design of the system in ref. 16) the fluidized bed could operate satisfactorily with a temperature ratio of about 3.5 and a thickness of about 1 meter. A Carnot cycle would have an efficiency of about 55 percent. If an actual efficiency of 0.7 of Carnot could be achieved, then the efficiency could be 38 percent. These results are comparable with those of reference 17 where it is suggested that a liquid metal might be required for such large heat fluxes.

The mass flow rate parameter is shown in figure 9(c). Immediately, one can see that approximately 10 times as much mass flow is required for the radiation-loss condition for the convection-loss condition for the porous copper. Also, for the heat flux of 640 kilowatts per square meter one can calculate that for air at a few atmospheres pressure a fluid velocity of a few meters per second is required for a fluidized bed. This is within the acceptable limits for bed design. Thus a fluidized bed may circumvent the need for a liquid-metal working fluid at high heat flux conditions.

CONCLUSIONS

The high effective conductivity of a fluidized bed makes it an attractive candidate as an absorber of thermal radiation for the purpose of heating an otherwise transparent fluid. The particle to gas heat-transfer coefficient is sufficiently large so that the temperature difference between the gas and the solid can be negligible. The longitudinal conductivity is much larger than the transverse conductivity, but the effect on the gas temperature can be counterracted by adjusting the other parameters. Finally, preliminary calculations for electric power systems on Earth indicate that the fluidized bed absorber could provide the required performance. Of course, some factors not considered in this ideal calculation could have a detrimental effect and would have to be considered for any actual applications. These include, among others, the effect of pressure drop in the collector on systems performance and the deterioration of the optical transmission through the transparent wall because of particle scratches or other contamination of the wall.

Lewis Research Center,
National Aeronautics and Space Administration,
Cleveland, Ohio, May 18, 1976,
506-24.

APPENDIX A

SYMBOLS

A	expansion coefficient defined in eq. (18)
a	expansion coefficient defined in eq. (11)
B	expansion coefficient defined in eq. (18)
b	expansion coefficient defined in eq. (12)
C	constant of integration defined in eq. (56)
c_p	specific heat
D	determinant of coefficients defined in eq. (28)
d	diameter
h	heat-transfer coefficient
k	thermal conductivity
L	length of porous media bed
M	expansion coefficient defined in eq. (26)
S	heat-transfer contact area between porous medium and gas
t	temperature
u	gas velocity
V	volume of porous media bed
x, z	coordinates shown in fig. 1
α	Eigenvalues defined in eq. (13)
β	heat-transfer coefficient parameter defined in eq. (15)
ϵ	emissivity
ζ	fraction of distance from entrance to exit of porous media
η	Carnot cycle efficiency
Θ	heat flux parameter defined in eq. (53)
μ	parallel thermal conductivity parameter defined in eq. (5)
ν	transverse thermal conductivity parameter defined in eq. (5)
ξ	fraction of distance from insulating wall to absorbing
ρ	gas density

σ Stefan-Boltzmann constant

Φ heat flux absorbed by porous media bed

φ dimensionless temperature of gas defined in eq. (4)

χ parameter defined in eq. (4)

ψ dimensionless temperature of porous media defined in eq. (4)

ω mass-flow parameter defined in eq. (5)

Subscripts:

coll collector

env environment

ex exit

g gas

max maximum

n, m summation indices

o entrance

s solid porous media

sx transverse

sz parallel

w wall

Superscripts:

(i) summation index

~ parameters and variables defined in appendix D for solution with no heat lost from absorbing surface

', '' first and second derivatives with respect to ζ

APPENDIX B

EVALUATION OF EIGENVALUES

It is necessary to find $\alpha_n(\nu)$ from equation (13):

$$\nu(\alpha_n) = \frac{1}{\alpha_n} \cot \alpha_n$$

The Newton-Raphson technique can be used if a good guess for the initial trial can be made. One which works can be found by replacing

$$\cot \alpha_n \quad \text{with} \quad \frac{\left(n + \frac{1}{2}\right)\pi - \alpha_n}{\alpha_n - n\pi}$$

This form has the correct zeroes and infinities. Then, the positive α_n root is

$$\alpha_n^t(\nu) = \frac{\sqrt{(1 + \nu n\pi)^2 + 2\nu\pi + (\nu n\pi - 1)}}{2\nu} \tag{B1}$$

The convergence of the Newton-Raphson technique is quicker if the logarithm of ν is taken:

$$\frac{d \ln \nu}{d\alpha_n} = -\frac{1}{\alpha_n} - \frac{1}{\sin \alpha_n \cos \alpha_n} \tag{B2}$$

Approximating the derivative by a difference and evaluating it at α_n^t result in

$$\frac{\ln \nu - \ln \dfrac{\cot \alpha_n^t}{\alpha_n^t}}{\alpha_n - \alpha_n^t} = -\frac{1}{\alpha_n^t} - \frac{1}{\sin \alpha_n^t \cos \alpha_n^t} \tag{B3}$$

Thus,

$$\alpha_n = \alpha_n^t - \frac{\ln \nu - \ln \dfrac{\cot \alpha_n^t}{\alpha_n^t}}{\dfrac{1}{\alpha_n^t} + \dfrac{1}{\sin \alpha_n^t \cos \alpha_n^t}} \tag{B4}$$

After each trial α_n^t is taken as the α_n. Convergence to any desired accuracy can be achieved. Obvious limiting forms are

$$\left.\begin{aligned} \lim_{\nu \to 0} \alpha_n &= \left(n + \frac{1}{2}\right)\pi \qquad n \neq 0 \\ \lim_{\nu \to \infty} \alpha_n &= n\pi \qquad n \neq 0 \end{aligned}\right\} \tag{B5}$$

APPENDIX C

ROOTS OF CUBIC EQUATION

Equation (20) can be rewritten as

$$\chi_n^3 - \left(\frac{\beta + \nu\alpha_n^2}{\mu} + \frac{\beta^2}{3\omega^2}\right)\chi_n + \frac{\beta}{3\omega}\left(\frac{2}{9}\frac{\beta^2}{\omega^2} + \frac{\beta}{\mu} - \frac{2\nu\alpha_n^2}{\mu}\right) = 0 \tag{C1}$$

where

$$\gamma_n = \chi_n - \frac{\beta}{3\omega} \tag{C2}$$

A convenient form to write the roots is achieved (ref. 18) by letting

$$\cos\varphi = \frac{-\frac{\beta}{6\omega}\left(\frac{2}{9}\frac{\beta^2}{\omega^2} + \frac{\beta - 2\nu\alpha_n^2}{\mu}\right)}{\frac{1}{3\sqrt{3}}\left(\frac{\beta^2}{3\omega^2} + \frac{\beta + \nu\alpha_n^2}{\mu}\right)^{3/2}} \tag{C3}$$

Then

$$\left.\begin{aligned}
\gamma_n^{(1)} &= \frac{2}{\sqrt{3}}\left(\frac{\beta^2}{3\omega^2} + \frac{\beta + \nu\alpha_n^2}{\mu}\right)^{1/2}\cos\frac{\varphi}{3} - \frac{\beta}{3\omega} \\
\gamma_n^{(2)} &= \frac{2}{\sqrt{3}}\left(\frac{\beta^2}{3\omega^2} + \frac{\beta + \nu\alpha_n^2}{\mu}\right)^{1/2}\cos\left(\frac{\varphi}{3} + \frac{2\pi}{3}\right) - \frac{\beta}{3\omega} \\
\gamma_n^{(3)} &= \frac{2}{\sqrt{3}}\left(\frac{\beta^2}{3\omega^2} + \frac{\beta + \nu\alpha_n^2}{\mu}\right)^{1/2}\cos\left(\frac{\varphi}{3} + \frac{4\pi}{3}\right) - \frac{\beta}{3\omega}
\end{aligned}\right\} \tag{C4}$$

Limiting forms:

(1)

$$\left.\begin{aligned} \lim_{\beta\to\infty} \gamma_n^{(1)} &= \frac{\omega}{2\mu}\left(1+\sqrt{1+\frac{4\mu\nu\alpha_n^2}{\omega^2}}\right) \\ \lim_{\beta\to\infty} \gamma_n^{(2)} &= -\infty \\ \lim_{\beta\to\infty} \gamma_n^{(3)} &= \frac{\omega}{2\mu}\left(1-\sqrt{1+\frac{4\mu\nu\alpha_n^2}{\omega^2}}\right) \end{aligned}\right\} \qquad \text{(C5)}$$

(2)

$$\left.\begin{aligned} \lim_{\mu\to\infty} \gamma_n^{(1)} &= 0 \\ \lim_{\mu\to\infty} \gamma_n^{(2)} &= -\frac{\beta}{\omega} \\ \lim_{\mu\to\infty} \gamma_n^{(3)} &= 0 \end{aligned}\right\} \qquad \text{(C6)}$$

(3)

$$\left.\begin{aligned} \lim_{\mu\to 0} \gamma_n^{(1)} &= \infty \\ \lim_{\mu\to 0} \gamma_n^{(2)} &= -\infty \\ \lim_{\mu\to 0} \gamma_n^{(3)} &= \frac{-\nu\alpha_n^2\beta}{\omega\left(\beta+\nu\alpha_n^2\right)} \end{aligned}\right\} \qquad \text{(C7)}$$

APPENDIX D

LIMITING SOLUTIONS

Infinite Conductivity of Porous Medium ($\nu \to \infty$; $\mu \to \infty$)

Equations (1) and (2) can be combined to yield an equation for the temperature of the gas:

$$(\rho u)_o c_p \frac{\partial t}{\partial z} = \frac{Sh_s}{V} (t_s - t) \tag{D1}$$

The energy balance on the porous medium requires

$$B(\rho u)_o c_p \left[t(L) - t(o)\right] = \left[\Phi - h_w(t_s - t_{env})\right] L \tag{D2}$$

where $t(o) = t_o$.

The solutions for the temperatures of the gas and the solid, using the parameters defined in equations (4) and (5) are

$$\varphi(\zeta) = e^{-\beta\zeta/\omega} + \psi(1 - e^{-\beta\zeta/\omega}) \tag{D3}$$

and

$$\psi = \frac{1 - e^{-\beta/\omega}}{\frac{1}{\omega} + 1 - e^{-\beta/\omega}} \tag{D4}$$

Infinite Conductivity of Porous Medium in the Direction Parallel to Flow ($\mu \to \infty$)

In this case the temperature of the porous medium is uniform in the z direction. Equations (1) and (2) can again be combined to provide a local heat balance for the fluid. (See eq. (D1).) However, in the porous medium the heat flux in the z direction is determined by the boundary condition. This condition can be introduced by integrating equation (1) over z.

$$(\rho u)_o c_p\left[t(\chi, L) - t(\chi, 0)\right] = k_{sx}\int_0^L \frac{\partial^2 t_s}{\partial x^2}\,dz + k_{sz}\left(\left.\frac{\partial t_s}{\partial z}\right|_{z=L} - \left.\frac{\partial t_s}{\partial z}\right|_{z=0}\right) \tag{D5}$$

Again, we require that no heat be conducted from either end of the porous medium, even as k_{sz} becomes infinite. Also, as k_{sz} becomes infinite t_s becomes a constant in the z direction. If the order of integration and differentiation is exchanged, then equation (D5) becomes

$$(\rho u)_o c_p\left[t(\chi, L) - t(\chi, 0)\right] = k_{sx} L \frac{d^2 L}{dx^2} \tag{D6}$$

Since t_s does not depend on z, equation (D1) can be integrated:

$$t = t_s + (t_s - t_o)e^{-\beta\zeta/\omega} \tag{D7}$$

This equation can be used to substitute for t in equation (D6), which can then be solved. The solution with $dt_s/dx = 0$ at $x = 0$ is

$$t_s = t_o(1 + C \cosh \chi\xi) \tag{D8}$$

where

$$\chi^2 \equiv \frac{\omega}{\nu}(1 - e^{-\beta/\omega}) \tag{D9}$$

The constant C must be determined from the boundary condition on the flux absorbing surface, as given in equation (3). In this case C is

$$C = \frac{\Phi + h_w(t_{env} - t_o)}{t_o h_w(\cosh \chi + \nu\chi \sinh \chi)} \tag{D10}$$

The solution can be written in terms of φ and ψ using equation (4) as

$$\varphi(\xi, \zeta) = 1 - \frac{\cosh \chi\xi(1 - e^{-\beta\zeta/\omega})}{\nu\chi \sinh \chi + \cosh \chi} \tag{D11}$$

$$\psi(\xi) = 1 - \frac{\cosh \chi\xi}{\nu\chi \sinh \chi + \cosh \chi} \tag{D12}$$

Infinite Conductivity of Porous Medium in Direction Transverse to Flow ($\nu \to \infty$)

In this case the temperature of the porous medium is uniform in the x direction. Equations (1) and (2) can again be combined to provide a local heat balance for the fluid:

$$(\rho u)_o c_p \frac{\partial t}{\partial z} = \frac{Sh_s}{V}(t_s - t) \tag{D1}$$

The heat balance for the porous media must be global in the x direction:

$$(\rho u)_o c_p \int_0^B \frac{\partial t}{\partial z}\, dx = k_{sx}\left(\left.\frac{\partial t_s}{\partial x}\right|_{x=B} - \left.\frac{\partial t_s}{\partial x}\right|_{x=0}\right) + k_{sz}\int_0^B \frac{\partial^2 t_s}{\partial z^2}\, dx$$

$$= \Phi - h_w\left[t_s(B,z) - t_{env}\right] + k_{sz}\int_0^B \frac{\partial^2 t_s}{\partial z^2}\, dx \tag{D13}$$

As k_{sx} becomes infinite the integrals can be evaluated. Substituting the variables defined in equations (4) and (15) into equation (41) results in

$$\omega \frac{d\varphi}{d\zeta} = \mu \frac{d^2\psi}{d\zeta^2} - \psi \tag{D14}$$

The solution to these equations are of the form

$$\varphi(\zeta) = \sum_{i=1}^{3} A_o^{(i)} e^{\gamma_o^{(i)}\zeta} \qquad \psi(\zeta) = \sum_{i=1}^{3} A_o^{(i)}\left[1 + \frac{\gamma_o^{(i)}\omega}{\beta}\right] e^{\gamma_o^{(i)}\zeta} \tag{D15}$$

where the $\gamma_o^{(i)}$ are given as the roots to

$$\omega\beta\gamma_o^{(i)} = \left[\gamma_o^{(i)}\omega + \beta\right]\left\{u\left[\gamma_o^{(i)}\right]^2 - 1\right\} \tag{D16}$$

and

$$\left.\begin{aligned} D_o A_o^{(1)} &= \gamma_o^{(2)}\left[\beta + \gamma_o^{(2)}\omega\right]\gamma_o^{(3)}\left[\beta + \gamma_o^{(3)}\omega\right]\left[e^{\gamma_o^{(3)}} - e^{\gamma_o^{(1)}}\right] \\ D_o A_o^{(2)} &= \gamma_o^{(1)}\left[\beta + \gamma_o^{(1)}\omega\right]\gamma_o^{(3)}\left[\beta + \gamma_o^{(3)}\omega\right]\left[e^{\gamma_o^{(1)}} - e^{\gamma_o^{(3)}}\right] \\ D_o A_o^{(3)} &= \gamma_o^{(1)}\left[\beta + \gamma_o^{(1)}\omega\right]\gamma_o^{(2)}\left[\beta + \gamma_o^{(2)}\omega\right]\left[e^{\gamma_o^{(2)}} - e^{\gamma_o^{(1)}}\right] \end{aligned}\right\} \tag{D17}$$

with

$$\begin{aligned} D_o \equiv\ & e^{\gamma_o^{(1)}}\gamma_o^{(1)}\left[\beta + \gamma_o^{(1)}\omega\right]\left[\gamma_o^{(3)} - \gamma_o^{(2)}\right]\left[\gamma_o^{(3)}\omega + \gamma_o^{(2)}\omega + \beta\right] \\ & + e^{\gamma_o^{(2)}}\gamma_o^{(2)}\left[\beta + \omega\gamma_o^{(2)}\right]\left[\gamma_o^{(1)} - \gamma_o^{(3)}\right]\left[\gamma_o^{(1)}\omega + \gamma_o^{(3)}\omega + \beta\right] \\ & + e^{\gamma_o^{(3)}}\gamma_o^{(3)}\left[\beta + \omega\gamma_o^{(3)}\right]\left[\gamma_o^{(2)} - \gamma_o^{(1)}\right]\left[\gamma_o^{(2)}\omega + \gamma_o^{(1)}\omega + \beta\right] \end{aligned} \tag{D18}$$

This is equivalent to setting $\nu\alpha_o^2 = 1$ and $\nu\alpha_n = 0$, where $n = 1, 2, \ldots$ in equation (13). In this case $M_o = 1$ and $M_n = 0$, where $n = 1, 2, \ldots$

Zero Heat Conductivity of Porous Media in Direction Parallel to Flow ($\mu \to 0$)

In this case $\mu = 0$ and the adiabatic boundary conditions at the entrance and exit to the porous media are satisfied. Then

$$\gamma_n^{(1)} = \infty \qquad \gamma_n^{(2)} = -\infty \qquad \gamma_n^{(3)} = \frac{-\beta\alpha_n^2\nu}{\omega\left(\beta + \nu\alpha_n^2\right)} \tag{D19}$$

and

$$\varphi = \sum_{n=0}^{\infty} M_n \exp - \frac{(\beta\nu\alpha_n^2\zeta)}{\left[\omega\left(\beta + \nu\alpha_n^2\right)\right]} \cos \alpha_n \xi \tag{D20}$$

$$\psi = \sum_{n=0}^{\infty} M_n \frac{\beta}{\beta + \nu\alpha_n^2} \exp - \frac{(\beta\nu\alpha_n^2\zeta)}{\left[\omega\left(\beta + \nu\alpha_n^2\right)\right]} \cos \alpha_n \xi \tag{D21}$$

Infinite Heat-Transfer Coefficient between Porous Media and Fluid ($\beta \to \infty$)

In this case $\beta \to \infty$. The mathematical difficulty occurs because the gas and porous medium temperature must be equal but the gas temperature of the entrance is arbitrary. This difficulty is handled by allowing the derivative to be infinite at one point - the entrance - so that the inlet gas temperature can be still used as a boundary condition (ref. 2). The $\gamma_n^{(i)}$ for this case are given in appendix C for $\zeta \neq 0$:

$$\varphi = \psi = \sum_{n=0}^{\infty} M_n \left\{ \frac{\gamma_n^{(3)} e^{\left[\gamma_n^{(3)} + \gamma_n^{(1)}\zeta\right]} - \gamma_n^{(1)} e^{\left[\gamma_n^{(1)} + \gamma_n^{(3)}\zeta\right]}}{\gamma_n^{(3)} e^{\gamma_n^{(3)}} - \gamma_n^{(1)} e^{\gamma_n^{(1)}}} \right\} \cos \alpha_n \xi \tag{D22}$$

No Heat Loss from Heated Surface ($h_w \to 0$)

In this case $h_w = 0$. The parameters used so far are defined with h_w in the denominator. New parameters must be defined:

$$\left.\begin{aligned} \tilde{\omega} \equiv \frac{\omega}{\nu} &= \frac{(\rho u)_o c_p B^2}{L k_{sx}} \qquad \tilde{\mu} = \frac{\mu}{\nu} = \frac{k_{sz}}{k_{sx}}\left(\frac{B}{L}\right)^2 \\ \tilde{\nu} \equiv \frac{1}{\nu} &= \frac{B h_w}{k_{sx}} \qquad \tilde{\beta} = \frac{\beta}{\nu} = \frac{Sh_s}{V}\frac{B^2}{k_{sx}} \end{aligned}\right\} \tag{D21}$$

The dependent variables used so far are defined so that they approach 1 as h_w becomes zero. New dependent variables must be defined:

$$\tilde{\varphi} \equiv \frac{(t - t_o)k_{sx}}{\Phi B} \qquad \tilde{\psi} \equiv \frac{(t_s - t_o)k_{sx}}{\Phi B} \tag{D22}$$

The new variables can be expressed in terms of the old:

$$\tilde{\varphi} = \left[1 - \frac{h_w(t_o - t_{env})}{\Phi}\right]\left(\frac{1 - \varphi}{\tilde{\nu}}\right) \tag{D23}$$

$$\tilde{\psi} = \left[1 - \frac{h_w(t_o - t_{env})}{\Phi}\right]\left(\frac{1 - \psi}{\tilde{\nu}}\right) \tag{D24}$$

The solutions when h_w approaches zero are

$$\tilde{\varphi} = \lim_{\tilde{\nu} \to 0} \frac{1}{\tilde{\nu}}(1 - \varphi) \tag{D25}$$

$$\tilde{\psi} = \lim_{\tilde{\nu} \to 0} \frac{1}{\tilde{\nu}}(1 - \psi) \tag{D26}$$

while holding $\tilde{\omega}$, $\tilde{\mu}$, and $\tilde{\beta}$ constant. To take these limits, substitute equation (21), (22), and (25) into equations (D25) and (D26):

$$\tilde{\varphi} = \lim_{\tilde{\nu}\to 0}\left\{\sum_{i=1}^{3}\frac{A_o^{(i)}}{\tilde{\nu}}\left[1 - e^{\gamma_o^{(i)}\zeta}\right]\cos\alpha_o\xi + \sum_{n=0}^{\infty}\sum_{i=1}^{3}\frac{A_n^{(i)}}{\tilde{\nu}}\left[1 - e^{\gamma_n^{(i)}\zeta}\right]\cos\alpha_n\xi\right\} \qquad \text{(D27)}$$

$$\tilde{\psi} = \lim_{\tilde{\nu}\to 0}\left\{\sum_{i=1}^{3}\frac{A_o^{(i)}}{\tilde{\nu}}\left[1 - \frac{\tilde{\beta} + \tilde{\omega}\gamma_o^{(i)}}{\tilde{\beta}}e^{\gamma_o^{(i)}\zeta}\right]\cos\alpha_o\xi\right.$$

$$\left. + \sum_{n=1}^{\infty}\sum_{i=1}^{3}\frac{A_n^{(i)}}{\tilde{\nu}}\left[1 - \frac{\tilde{\beta} + \tilde{\omega}\gamma_n^{(i)}}{\tilde{\beta}}e^{\gamma_n^{(i)}\zeta}\right]\cos\alpha_n\xi\right\} \qquad \text{(D28)}$$

The term $n = 0$ has been taken out of the summation because it must be handled separately in the limiting process.

Consider first the terms for $n = 0$. From equation (13) one has

$$\alpha_o = 0$$

and from equation (20)

$$\left.\begin{aligned}
\lim_{\tilde{\nu}\to 0}\gamma_o^{(1)} &= \frac{\tilde{\beta}}{2\tilde{\omega}}\left(-1 + \sqrt{1 + \frac{4\tilde{\omega}^2}{\tilde{\mu}\tilde{\beta}}}\right)\\
\lim_{\tilde{\nu}\to 0}\gamma_o^{(2)} &= \frac{\tilde{\beta}}{2\tilde{\omega}}\left(-1 - \sqrt{1 + \frac{4\tilde{\omega}^2}{\tilde{\mu}\tilde{\beta}}}\right)\\
\lim_{\tilde{\nu}\to 0}\frac{\gamma_o^{(3)}}{\tilde{\nu}} &= -\frac{1}{\tilde{\omega}}
\end{aligned}\right\} \qquad \text{(D29)}$$

From equations (26) and (28)

$$M_o = 1$$

$$D_o = \gamma_o^{(1)}\gamma_o^{(2)}\left[\tilde{\beta} + \tilde{\omega}\gamma_o^{(1)}\right]\left[\tilde{\beta} + \tilde{\omega}\gamma_o^{(2)}\right]\left[e^{\gamma_o^{(2)}} - e^{\gamma_o^{(1)}}\right]$$

Substituting these values into equations (27) makes it possible to take the limits

$$\left.\begin{aligned}
\lim_{\tilde{\nu}\to 0} \frac{A_o^{(1)}}{\tilde{\nu}} &= -\frac{\tilde{\beta}}{\tilde{\omega}} \frac{\left[1 - e^{-\gamma_o^{(2)}}\right]}{\gamma_o^{(1)}\left[\tilde{\beta} + \tilde{\omega}\gamma_o^{(1)}\right]}\left[e^{\gamma_o^{(2)}} - e^{\gamma_o^{(1)}}\right] \\
\lim_{\tilde{\nu}\to 0} \frac{A_o^{(2)}}{\tilde{\nu}} &= -\frac{\tilde{\beta}}{\tilde{\omega}} \frac{\left[e^{\gamma_o^{(1)}} - 1\right]}{\gamma_o^{(2)}\left[\tilde{\beta} + \tilde{\omega}\gamma_o^{(2)}\right]\left[e^{\gamma_o^{(2)}} - e^{\gamma_o^{(1)}}\right]} \\
\lim_{\tilde{\nu}\to 0} \frac{A_o^{(3)}}{\tilde{\nu}}\left[1 - e^{\gamma_o^{(3)}\zeta}\right] &= \frac{\zeta}{\tilde{\omega}} \\
\lim_{\tilde{\nu}\to 0} \frac{A_o^{(3)}}{\tilde{\nu}}\left[1 - \frac{\tilde{\beta} + \tilde{\omega}\gamma_o^{(3)}}{\tilde{\beta}} e^{\gamma_o^{(3)}\zeta}\right] &= \frac{1}{\tilde{\beta}} + \frac{\zeta}{\tilde{\omega}}
\end{aligned}\right\} \qquad \text{(D30)}$$

With these values and making use of the equations for $\gamma_o^{(1)}$, $\gamma_o^{(2)}$, equations (D27) and (D28) may be written:

$$\tilde{\varphi} = \frac{\zeta}{\tilde{\omega}} + \frac{\tilde{\mu}}{\tilde{\omega}^2}\left\{1 + \frac{\left[1 - e^{\gamma_o^{(2)}}\right]e^{\gamma_o^{(1)}\zeta} + \left[e^{\gamma_o^{(1)}} - 1\right]e^{\gamma_o^{(2)}\zeta}}{e^{\gamma_o^{(2)}} - e^{\gamma_o^{(1)}}}\right\}$$

$$+ \lim_{\tilde{\nu}\to\infty} \sum_{n=1}^{\infty} \sum_{i=1}^{3} \frac{A_n^{(2)}}{\tilde{\nu}}\left[1 - e^{\gamma_n^{(2)}\zeta}\right] \cos \alpha_n \xi \qquad \text{(D31)}$$

$$\tilde{\psi} = \frac{1}{\tilde{\beta}} + \frac{\zeta}{\tilde{\omega}} + \frac{1}{\tilde{\omega}}\left\{\frac{\tilde{\mu}}{\tilde{\omega}} + \frac{\left[1 - e^{\gamma_o^{(2)}}\right]e^{\gamma_o^{(1)}\zeta}}{\gamma_o^{(1)}\left[e^{\gamma_o^{(2)}} - e^{\gamma_o^{(1)}}\right]} + \frac{\left[e^{\gamma_o^{(1)}} - 1\right]e^{\gamma_o^{(2)}\zeta}}{\gamma_o^{(2)}\left[e^{\gamma_o^{(2)}} - e^{\gamma_o^{(1)}}\right]}\right\}$$

$$+ \lim_{\nu\to\infty} \sum_{n=1}^{\infty} \sum_{i=1}^{3} \frac{A_n^{(i)}}{\tilde{\nu}}\left[1 - \frac{\tilde{\beta} + \tilde{\omega}\gamma_n^{(i)}}{\tilde{\beta}} e^{\gamma_n^{(i)}\zeta}\right] \cos \alpha_n \xi \qquad \text{(D32)}$$

The terms for n greater than zero offer no special difficulty if one evaluates M_n from equation (26) and α_n from equation (13) as $\tilde{\nu}$ becomes zero:

$$\lim_{\tilde{\nu}\to 0} \frac{M_n}{\tilde{\nu}} = \frac{2(-1)^n}{n^2\pi^2} \qquad \lim_{\tilde{\nu}\to 0} \alpha_n = n\pi$$

With this evaluation of M_n, the α_n and the $\gamma_n^{(i)}$ defined as the three roots of

$$\tilde{\mu}\tilde{\beta}\gamma_n = (\tilde{\beta} + \tilde{\omega}\gamma_n)(\tilde{\mu}\gamma_n^2 - n^2\pi^2) \qquad \text{(D34)}$$

and the $A_n^{(i)}$ defined in equations (27) and (38), then the limits in equations (D31) and (D32) can be taken. The solutions given in those equations are the analytical solutions to the problem solved numerically by Koh and Colony (ref. 8). The solution in

equation (D28) converges faster if one makes use of the fact that

$$\frac{\xi^2}{2} - \frac{1}{6} = \sum_{n=1}^{\infty} \lim_{\tilde{\nu} \to 0} \sum_{i=1}^{\infty} \frac{A_n^{(i)}}{\tilde{\nu}} \cos n\pi\xi$$

since from equation (26):

$$\lim_{\tilde{\nu} \to 0} \sum_{i=1}^{\infty} \frac{A_n^{(i)}}{\tilde{\nu}} = \lim_{\tilde{\nu} \to 0} \frac{M_n}{\tilde{\nu}} = \frac{2(-1)^n}{n^2 \pi 2}$$

REFERENCES

1. Lewis, W. K.; Gilliland, E. R.; and Girouard, H.: Heat Transfer in Solids Mixing in Beds of Fluidized Solids. Chem. Eng. Progr., Symp. Ser., vol. 58, no. 38, 1962, pp. 87-97.

2. Bland, D. R.: Mathematical Theory of the Flow of a Gas in a Porous Solid and of the Associated Temperature Distributions. Proc. Roy. Soc. (London), Ser. A, vol. 221, no. 1144, Jan. 1954, pp. 1-28.

3. Grootenhuis, P.: The Mechanism and Application of Effusion Cooling. The J. Roy. Aeron. Soc., vol. 63, no. 578, Mar. 1958, pp. 73-89.

4. Lasseter, T. J.: The Numerical Simulation of Heat and Mass Transfer in Multi-Dimensional Two-Phase Geothermal Reservoirs. ASME Paper 75-WA/HT-71, Aug. 1975.

5. Ribando, R. J.; and Torrance, K. E.: Natural Convection in a Porous Medium, Effects of Confinement, Variable Permeability and Thermal Boundary Conditions. ASME Paper 75-WA/HT-73, Aug. 1975.

6. Siegel, Robert; and Goldstein, Marvin E.: Analytical Method for Steady State Heat Transfer in Two Dimensional Porous Media. NASA TN D-5878, 1970.

7. Siegel, Robert: Conformal Mapping Technique for Two-Dimensional Porous Media and Jet Impingement Heat Transfer. NASA TM X-68276, 1974.

8. Koh, J. C. Y.; and Colony, R.: Analysis of Cooling Effectiveness for Porous Material in a Coolant Passage. Trans. ASME, vol. 96, Aug. 1974, pp. 324-330.

9. Jakob, Max: Heat Transfer. Vol. II, John Wiley & Sons, Inc., 1957.

10. Eckert, Ernst R. G.; and Drake, Robert M., Jr.: Analysis of Heat and Mass Transfer. McGraw-Hill Book Co., Inc., 1972.

11. Deissler, R. G.; and Boegli, J. S.: An Investigation of Effective Thermal Conductivities of Powders in Various Gases. Trans. ASME, vol. 80, Oct. 1958, pp. 1417-1425.

12. Bayley, F. J.; and Turner, A. B.: The Transpiration-Cooled Gas Turbine. J. Eng. Power, vol. 92, no. 4, Oct. 1970, pp. 351-358.

13. Kunii, Daizo; and Levenspiel, Octave: Fluidization Engineering. John Wiley & Sons, Inc., 1969.

14. Koh, J. C. Y.; and Fortini, Anthony: Prediction of Thermal Conductivity and Electrical Resistivity of Porous Metallic Materials. Intern. J. Heat Mass Transfer, vol. 16, no. 10, Oct. 1973, pp. 2013-2022.

15. Jakob, Max: Heat Transfer. Vol. I, John Wiley & Sons, Inc., 1949.

16. Riaz, M.: A Theory of Concentrators of Solar Energy on a Central Receiver for Electric Power Generation. ASME Paper 75-WA/Sol-1, Jul. 1975.

17. Hildebrandt, A. F.; and Vaunt-Hull, L. L. L.: A Tower Top Focus Solar Energy Collector. ASME Paper 73-WA/Sol-7, July, 1973.

18. Handbook of Chemistry and Physics. 47th ed., Chemical Rubber Co., 1966, p. A-235.

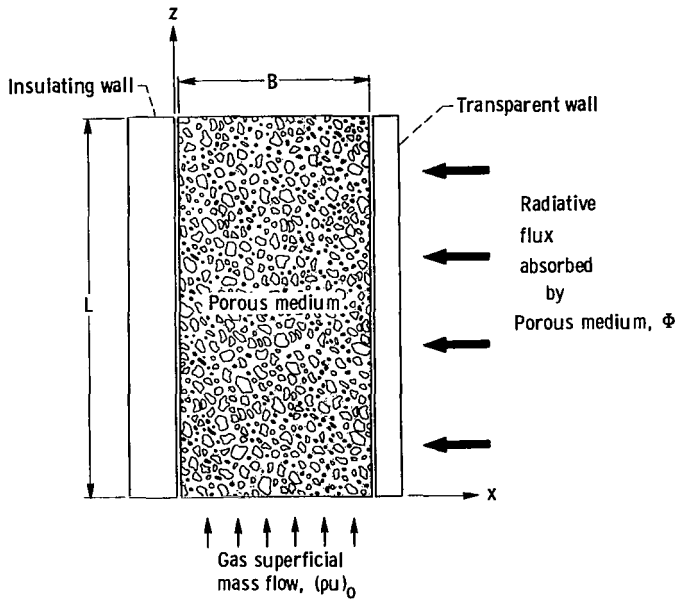

Figure 1. - Schematic diagram of porous media absorber.

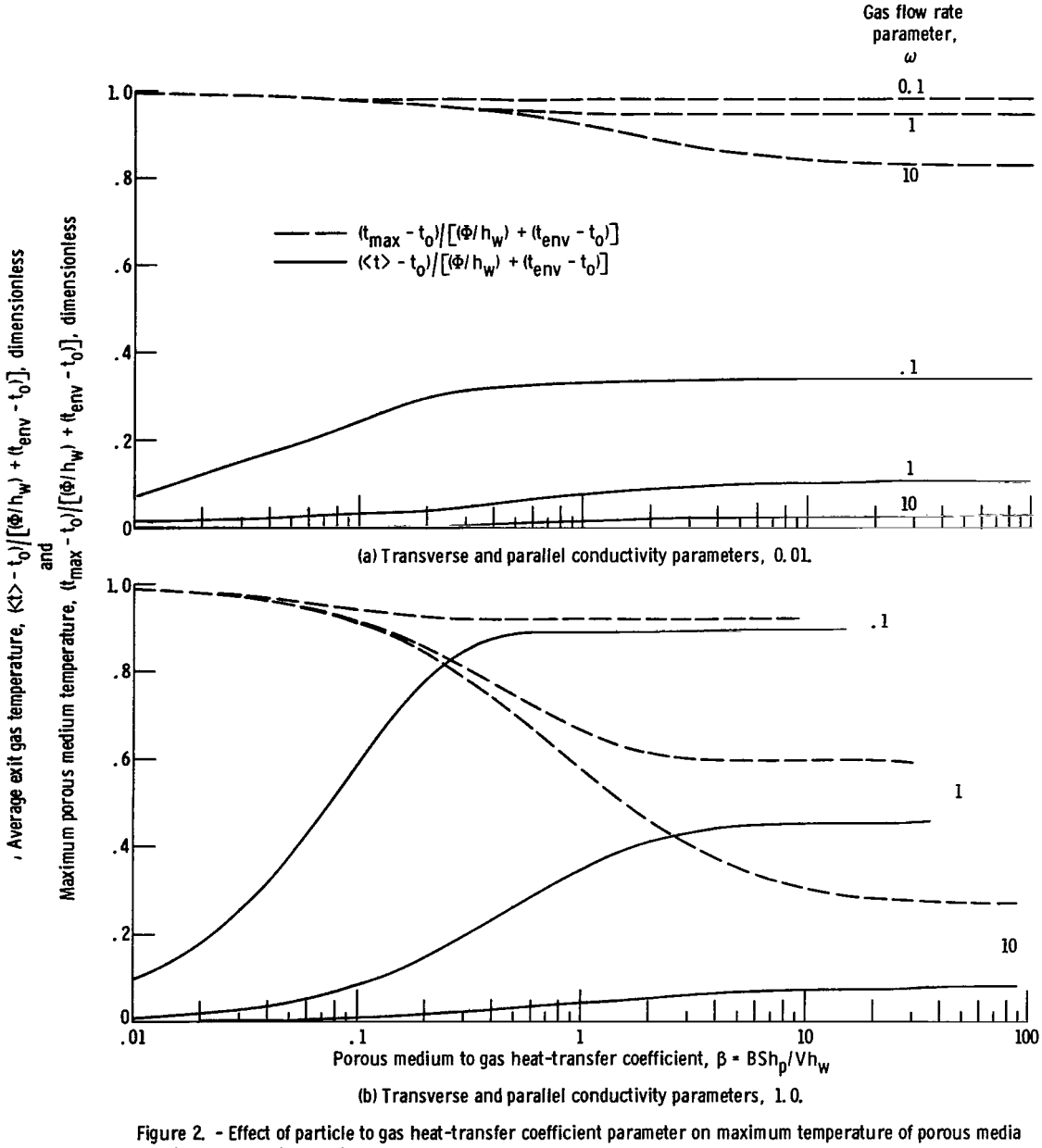

(a) Transverse and parallel conductivity parameters, 0.01.

(b) Transverse and parallel conductivity parameters, 1.0.

Figure 2. - Effect of particle to gas heat-transfer coefficient parameter on maximum temperature of porous media and average gas temperature.

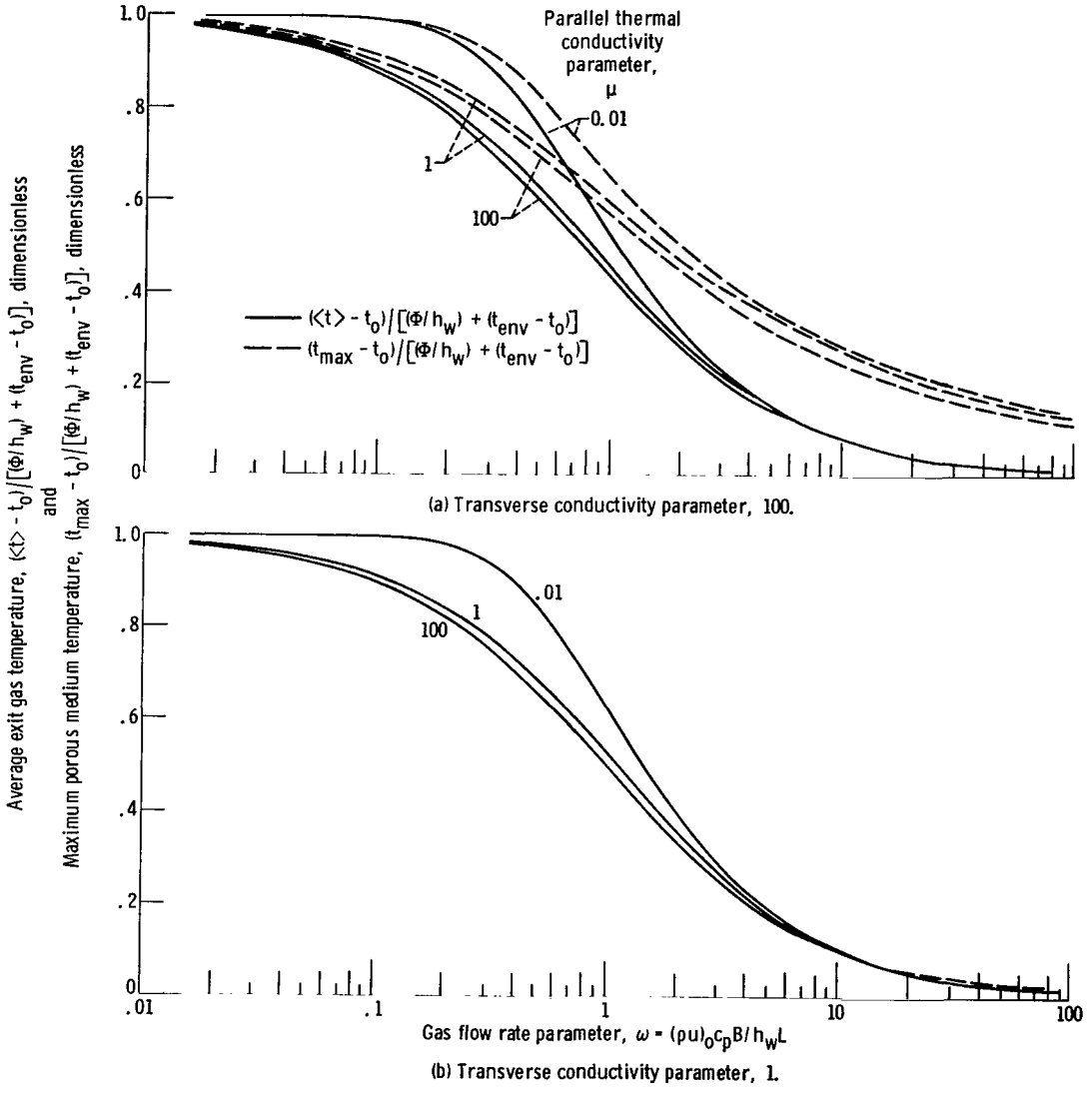

Figure 3. - Effect of mass flow and axial heat conduction on average exit gas temperature and maximum porous medium temperature. Particle to gas heat transfer parameter, 100.

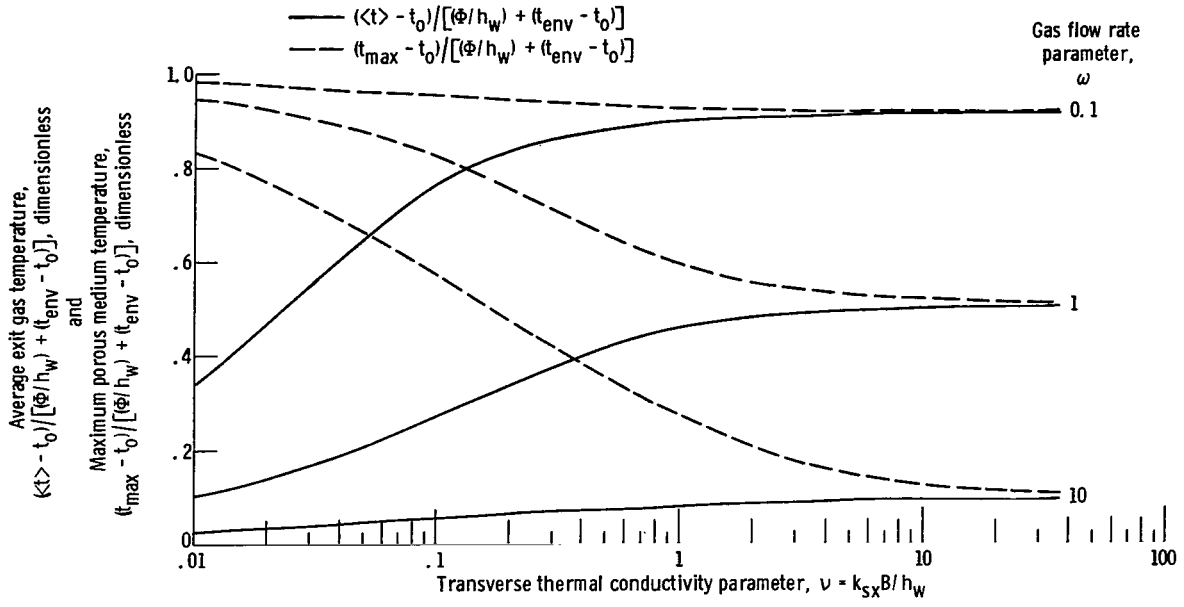

Figure 4. - Effect of transverse and parallel conductivity parameter on maximum temperature of porous media and average gas temperature. Particle to gas heat-transfer coefficient parameter, 100; transverse and parallel thermal conductivity parameters are equal.

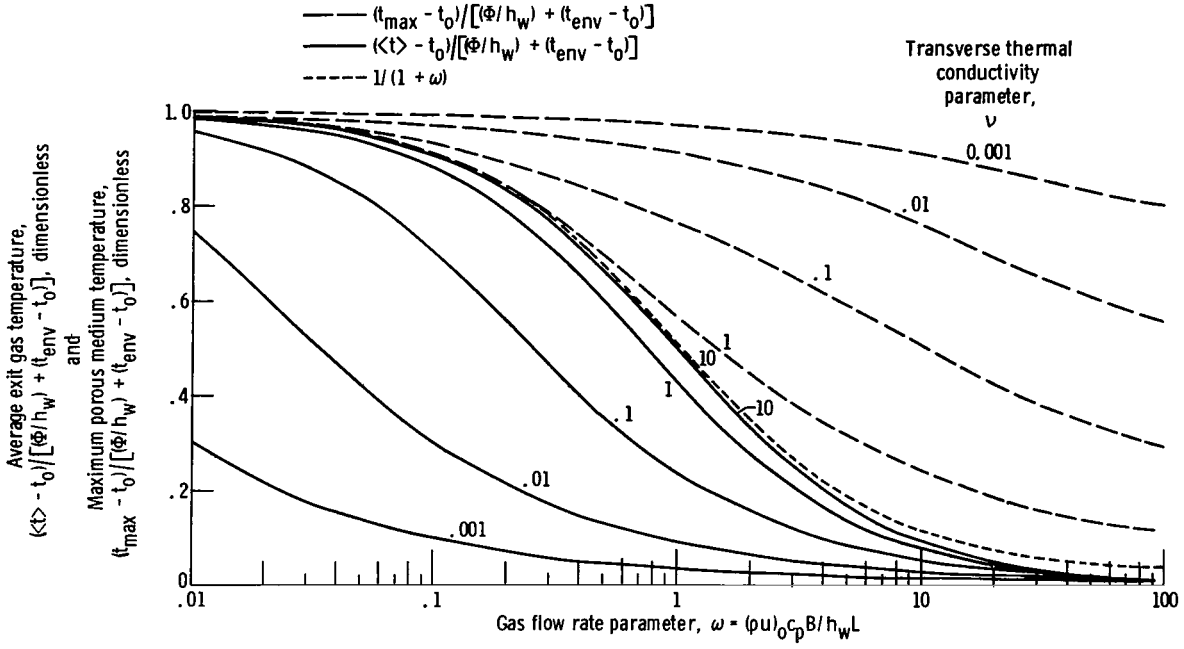

Figure 5. - Effect of gas flow rate parameter on maximum temperature of porous media and average exit gas temperature. Parallel conductivity parameter is infinite; porous media to gas heat transfer coefficient parameter, 100.

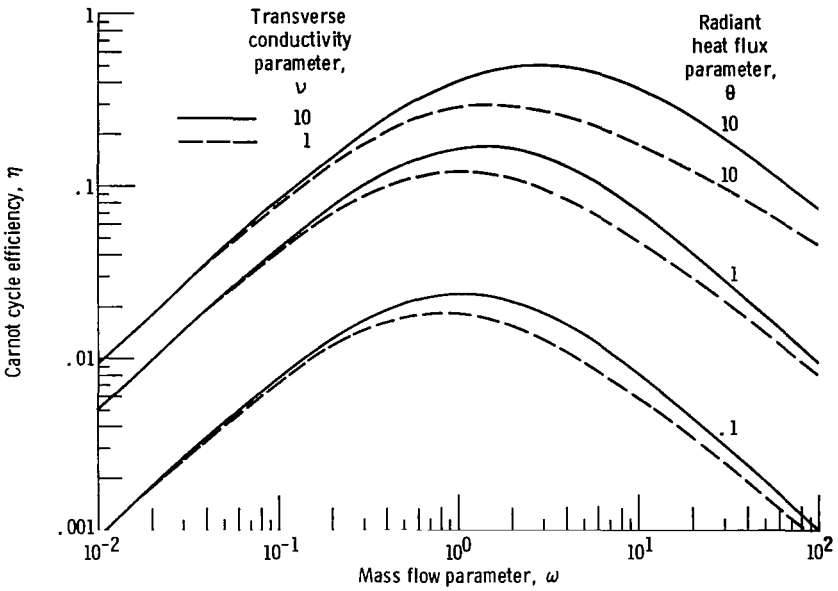

Figure 6. - Effect of mass flow parameter on Carnot cycle efficiency for collector with heat loss by convection. Porous medium to gas heat transfer coefficient parameter, 100; parallel conductivity parameter is infinite.

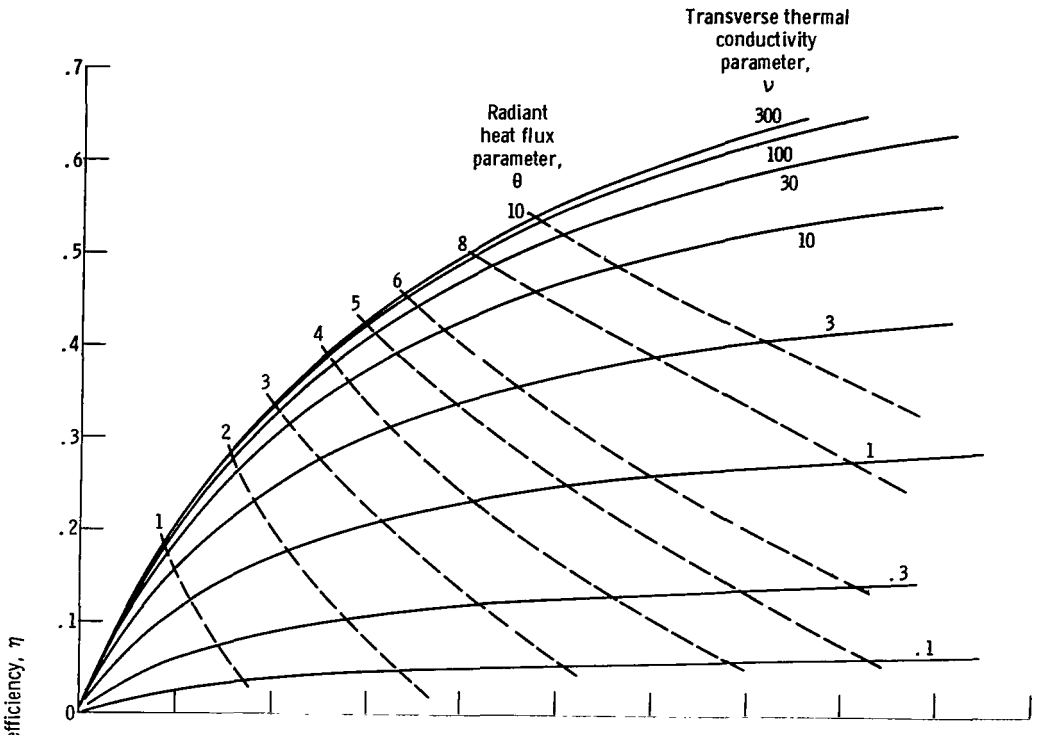

(a) All collector heat loss to environment by convection.

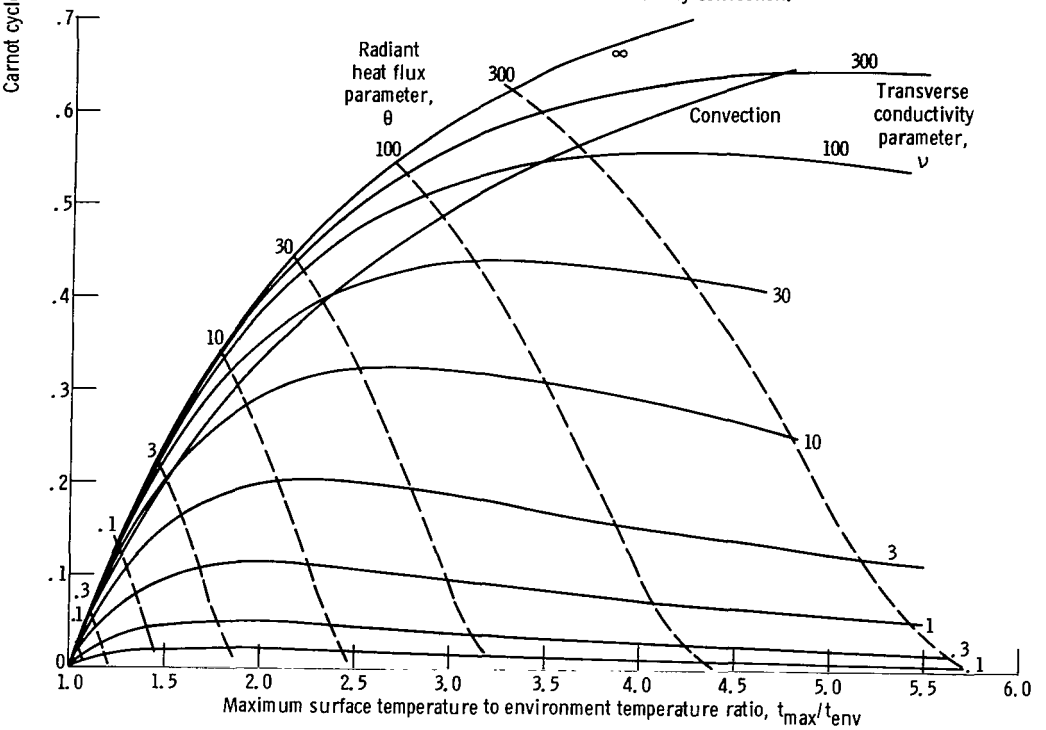

(b) All collector heat loss to environment by radiation only (except for curve marked "convection," which corresponds to collector losses by convection and with infinite transverse conductivity. The θ and ν values do not apply to this curve.)

Figure 7. - Carnot cycle efficiency as function of maximum surface temperature to environment temperature ratio.

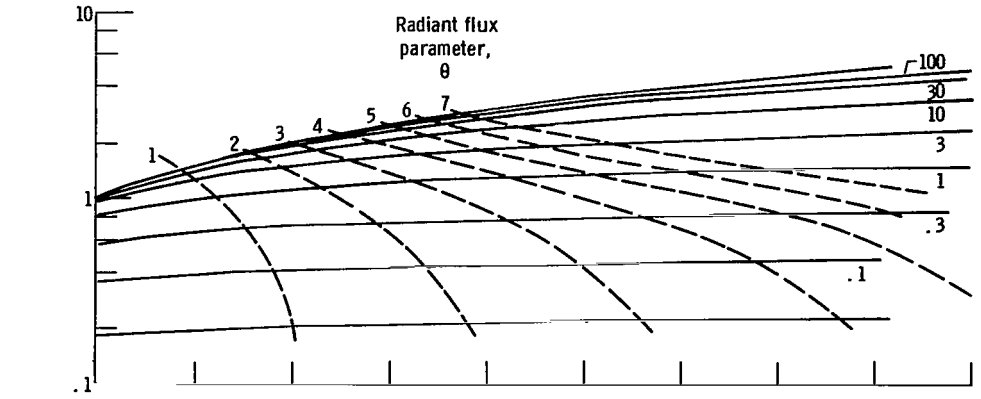

(a) Collector losses to environment by convection only.

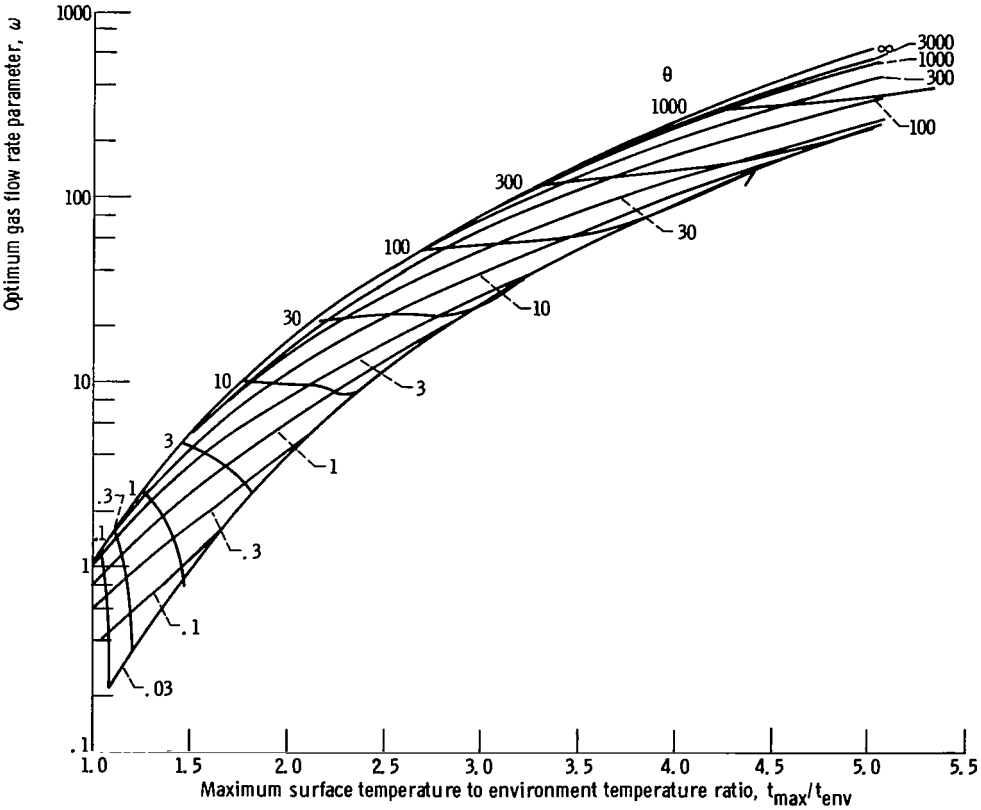

(b) Collector losses to environment by radiation only.

Figure 8. - Effect of surface temperature to environment temperature ratio on optimum mass flow parameter.

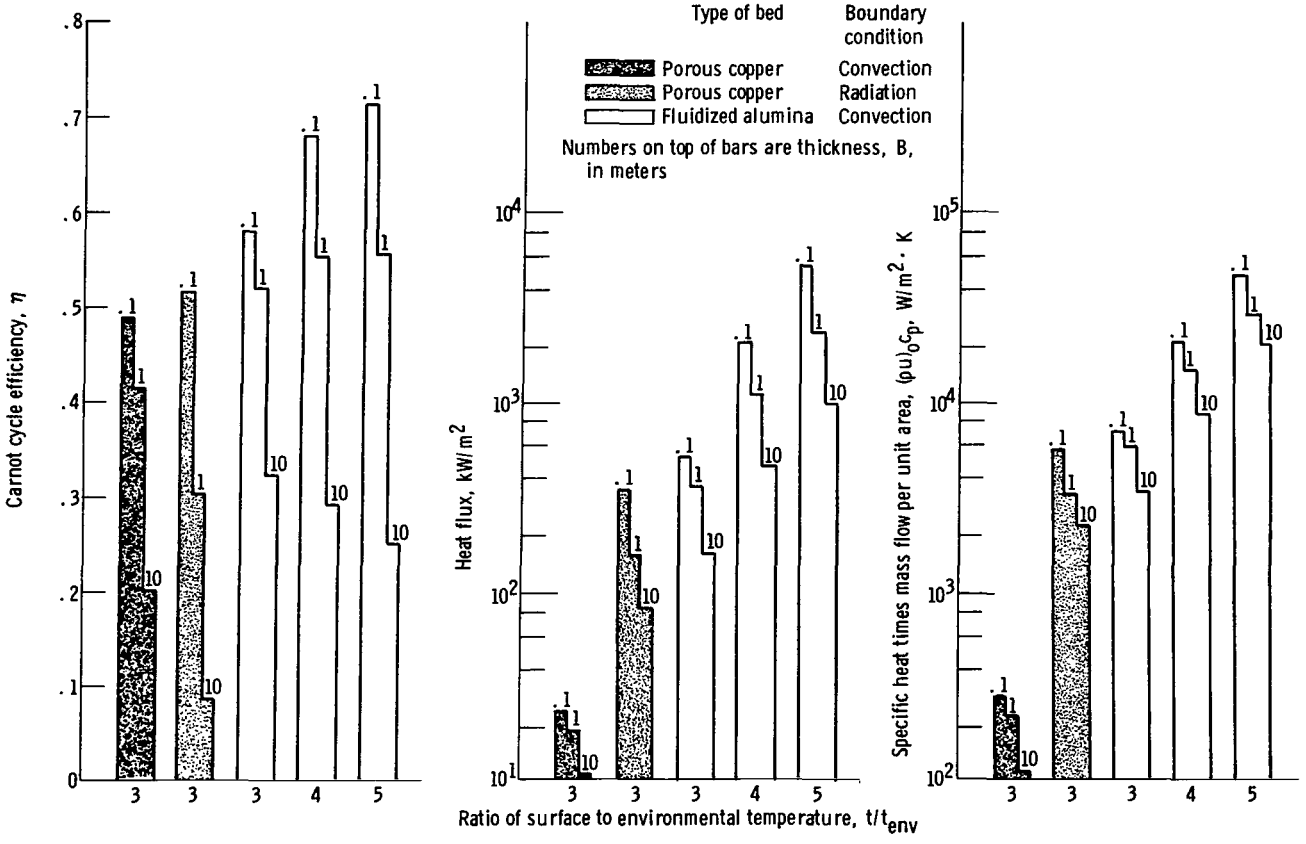

Figure 9. - Comparison of performance parameters for collectors with length to thickness ratios of 10.

NATIONAL AERONAUTICS AND SPACE ADMINISTRATION
WASHINGTON, D.C. 20546

OFFICIAL BUSINESS
PENALTY FOR PRIVATE USE $300

SPECIAL FOURTH-CLASS RATE
BOOK

POSTAGE AND FEES PAID
NATIONAL AERONAUTICS AND
SPACE ADMINISTRATION
451

U.S.MAIL

783 001 C1 U D 760916 S00903DS
DEPT OF THE AIR FORCE
AF WEAPONS LABORATORY
ATTN: TECHNICAL LIBRARY (SUL)
KIRTLAND AFB NM 87117

POSTMASTER: If Undeliverable (Section 158 Postal Manual) Do Not Return

"The aeronautical and space activities of the United States shall be conducted so as to contribute . . . to the expansion of human knowledge of phenomena in the atmosphere and space. The Administration shall provide for the widest practicable and appropriate dissemination of information concerning its activities and the results thereof."

—NATIONAL AERONAUTICS AND SPACE ACT OF 1958

NASA SCIENTIFIC AND TECHNICAL PUBLICATIONS

TECHNICAL REPORTS: Scientific and technical information considered important, complete, and a lasting contribution to existing knowledge.

TECHNICAL NOTES: Information less broad in scope but nevertheless of importance as a contribution to existing knowledge.

TECHNICAL MEMORANDUMS: Information receiving limited distribution because of preliminary data, security classification, or other reasons. Also includes conference proceedings with either limited or unlimited distribution.

CONTRACTOR REPORTS: Scientific and technical information generated under a NASA contract or grant and considered an important contribution to existing knowledge.

TECHNICAL TRANSLATIONS: Information published in a foreign language considered to merit NASA distribution in English.

SPECIAL PUBLICATIONS: Information derived from or of value to NASA activities. Publications include final reports of major projects, monographs, data compilations, handbooks, sourcebooks, and special bibliographies.

TECHNOLOGY UTILIZATION PUBLICATIONS: Information on technology used by NASA that may be of particular interest in commercial and other non-aerospace applications. Publications include Tech Briefs, Technology Utilization Reports and Technology Surveys.

Details on the availability of these publications may be obtained from:

SCIENTIFIC AND TECHNICAL INFORMATION OFFICE

NATIONAL AERONAUTICS AND SPACE ADMINISTRATION

Washington, D.C. 20546